

# Symmetry-resolved elastic anomalies in spin-crossover cobaltite $\text{LaCoO}_3$

T. Watanabe<sup>1,\*</sup>, R. Okada<sup>1</sup>, and K. Tomiyasu<sup>2†</sup>

<sup>1</sup>*Department of Physics, College of Science and Technology,  
Nihon University, Chiyoda, Tokyo 101-8308, Japan and*

<sup>2</sup>*Department of Physics, Tohoku University, Sendai, Miyagi 980-8577, Japan*

(Dated: May 27, 2022)

Ultrasound velocity measurements of the pseudo-cubic spin-crossover cobaltite  $\text{LaCoO}_3$  and the lightly Ni-doped  $\text{La}(\text{Co}_{0.99}\text{Ni}_{0.01})\text{O}_3$  reveal two types of symmetry-resolved elastic anomaly in the insulating paramagnetic state that are commonly observed in these compounds. The temperature dependence of the bulk modulus exhibits Curie-type softening upon cooling below 300 K down to  $\sim 70$  K, indicating the presence of isostructural lattice instability arising from magnetic fluctuations. The temperature dependence of the tetragonal and trigonal shear moduli exhibits unusual hardening upon cooling below 300 K, indicating the occurrence of elasticity crossover arising from the spin crossover. The present study also reveals that the isostructural lattice instability in  $\text{LaCoO}_3$  is suppressed by the Ni doping, indicating the suppression of the magnetic fluctuations by the Ni doping in conjunction with the enhancement of electron itinerancy. This Ni doping effect in  $\text{LaCoO}_3$  can be explained on the basis that the isostructural lattice instability arises from the coupling of the lattice to the Co spin state fluctuating between the high-spin state and intermediate-spin state.

PACS numbers:

## I. INTRODUCTION

Transition-metal oxides have attracted great interest owing to the emergence of rich and exotic electronic phenomena that arise from strong electron correlations [1]. Perovskite cobaltite  $\text{LaCoO}_3$  is a unique correlated system with spin-state degrees of freedom that exhibits thermally induced two-step crossovers of the Co spin state; i.e., upon heating, the nonmagnetic insulating ground state changes first to a paramagnetic insulating state at approximately 100 K and then second to a paramagnetic metallic state at approximately 500 K [2,3].

Spin crossover between low-spin (LS) and high-spin (HS) states of transition-metal ions occurs in a wide range of materials, the majority of which are molecular complexes [4–10].  $\text{LaCoO}_3$  is known to be a prototypical spin-crossover material but a rare solid-crystalline one, where the Co spin state is expected to be affected by the inter-Co-site interactions as well as the coupling between the electronic and lattice degrees of freedom. Regarding the thermally induced spin crossover of  $\text{LaCoO}_3$  at  $\sim 100$  K, it has long been debated whether the thermally excited state is an HS state ( $t_{2g}^4 e_g^2$ ,  $S = 2$ ) [11–20] or intermediate-spin (IS) state ( $t_{2g}^5 e_g^1$ ,  $S = 1$ ) [21–25].

In the insulating paramagnetic state of  $\text{LaCoO}_3$  at temperatures between  $\sim 100$  K and  $\sim 500$  K, short-range ferromagnetic correlation has been observed for spin-state excitations in neutron scattering experiments [14,26,27]. It has recently been claimed that this ferromagnetic correlation emerges in the nearest-neighbor  $\text{Co}^{3+}$  pairs; i.e., the spin-state pair fluctuates between the HS-LS paired state and IS-IS paired state, which is called the HS-IS duality of the magnetic  $\text{Co}^{3+}$  ions [28,29]. For this HS-IS duality, it has additionally been claimed that the spatial correlation scale is on the order of seven Co sites comprising one central Co site and its six nearest-

neighbor Co sites, and the Co-3d electrons are fairly delocalized within this seven-site unit [28]. For the emergence of the HS-IS duality, Co-O covalency might play a role [30]. The HS-IS duality indicates that the Co spin state of  $\text{LaCoO}_3$  is strongly affected by the inter-Co-site interactions, which sheds light on the long-standing controversy over HS and IS states under the conventional one-Co-site classification. Very recently, high-magnetic-field magnetostriction studies on  $\text{LaCoO}_3$  revealed the emergence of magnetic-field-induced multiple spin-state phases at high magnetic fields above  $\sim 70$  T and temperatures below  $\sim 100$  K, and it has been claimed that these phases originate from the HS-IS duality [31,32].

In the solid-crystalline  $\text{LaCoO}_3$ , the Co spin state is expected to be effected by not only the inter-Co-site interactions but also the coupling between the electronic and lattice degrees of freedom. We herein study the interplay of spin-state and lattice degrees of freedom in the spin-crossover cobaltite  $\text{LaCoO}_3$  by means of ultrasound velocity measurements for a single crystal, which are a measure of the elastic moduli of this pseudo-cubic compound. The elastic modulus of a crystal is a thermodynamic tensor quantity, and the ultrasound velocity measurements of the symmetrically independent elastic moduli of a crystal thus provide symmetry-resolved thermodynamic information. In magnets, the modified sound dispersions caused by magnetoelastic coupling allow the extraction of detailed information on the interplay of the lattice and electronic degrees of freedom [33–48]. For  $\text{LaCoO}_3$ , it has been reported that the longitudinal sound velocity along the cubic [111] direction has an unusual temperature dependence, which should arise from the spin crossover [48]. The present study investigates the elastic properties of  $\text{LaCoO}_3$  for all symmetrically independent elastic moduli of the cubic crystal, namely the bulk modulus  $C_B$ , tetragonal shear modulus  $\frac{C_{11}-C_{12}}{2}$ , and trigonal shear modulus  $C_{44}$ .

In the present study, we measure ultrasound velocities for single crystals of not only  $\text{LaCoO}_3$  but also lightly Ni-doped  $\text{La}(\text{Co}_{0.99}\text{Ni}_{0.01})\text{O}_3$ . For the Ni-doped  $\text{LaCoO}_3$  of  $\text{La}(\text{Co}_{1-x}\text{Ni}_x)\text{O}_3$ , it is known that the electrical resistivity rapidly decreases with an increasing Ni concentration  $x$  only below a few percent, which is considered to enable the insulator-to-metal transition at  $x \sim 0.4$  [49].  $\text{LaCoO}_3$  and  $\text{La}(\text{Co}_{0.99}\text{Ni}_{0.01})\text{O}_3$  are both semiconductors, but the electrical resistivity of  $\text{La}(\text{Co}_{0.99}\text{Ni}_{0.01})\text{O}_3$  is much lower than that of  $\text{LaCoO}_3$ , indicating that the Ni-doping sensitively enhances the electron itinerancy [50]. By comparing the elastic properties of  $\text{LaCoO}_3$  and  $\text{La}(\text{Co}_{0.99}\text{Ni}_{0.01})\text{O}_3$ , we examine how the controversial Co spin state of the insulating paramagnetic  $\text{LaCoO}_3$  and its coupling to the lattice are affected by the enhancement of electron itinerancy.

## II. EXPERIMENTAL

Single crystals of  $\text{LaCoO}_3$  and  $\text{La}(\text{Co}_{0.99}\text{Ni}_{0.01})\text{O}_3$  were prepared using the floating-zone method [50]. The ultrasound velocities were measured adopting the phase-comparison technique with longitudinal and transverse sound waves at a frequency of 30 MHz. The ultrasound waves were generated and detected by  $\text{LiNbO}_3$  transducers glued to parallel mirror surfaces of the crystal. Measurements were made to determine the symmetrically independent elastic moduli of the pseudo-cubic crystal, specifically the compression modulus  $C_{11}$ , tetragonal shear modulus  $\frac{C_{11}-C_{12}}{2} \equiv C_t$ , and trigonal shear modulus  $C_{44}$ . From  $C_{11}$  and  $C_t$  data, we also obtained the bulk modulus  $C_B = \frac{C_{11}+2C_{12}}{3} = C_{11} - \frac{4}{3}C_t$ . For the pseudo-cubic crystal,  $C_{11}$ ,  $C_t$ , and  $C_{44}$  were respectively measured using longitudinal ultrasound with propagation  $\mathbf{k} \parallel [100]$  and polarization  $\mathbf{u} \parallel [100]$ , transverse ultrasound with  $\mathbf{k} \parallel [110]$  and  $\mathbf{u} \parallel [1\bar{1}0]$ , and transverse ultrasound with  $\mathbf{k} \parallel [110]$  and  $\mathbf{u} \parallel [001]$ . The sound velocities of  $\text{LaCoO}_3$  ( $\text{La}(\text{Co}_{0.99}\text{Ni}_{0.01})\text{O}_3$ ) measured at 300 K are  $\sim 3970$  m/s ( $\sim 5120$  m/s) for  $C_{11}$ ,  $\sim 2760$  m/s ( $\sim 3060$  m/s) for  $C_t$ , and  $\sim 2680$  m/s ( $\sim 3370$  m/s) for  $C_{44}$ .

## III. RESULTS AND DISCUSSION

Figures 1(a)–1(c) respectively present the temperature ( $T$ ) dependence of the elastic moduli  $C_B(T)$ ,  $C_t(T)$ , and  $C_{44}(T)$  for  $\text{LaCoO}_3$ . Here,  $C_B(T) = C_{11}(T) - \frac{4}{3}C_t(T)$  is obtained from  $C_{11}(T)$  [the inset in Fig. 1(a)] and  $C_t(T)$  [Fig. 1(b)]. Among the elastic moduli shown in Figs. 1(a)–1(c), the bulk modulus  $C_B(T)$  [Fig. 1(a)] exhibits huge Curie-type ( $\sim -1/T$ -type) softening upon cooling from 300 K to  $\sim 70$  K with the magnitude of  $\Delta C_B/C_B$  being  $\sim 50$  %, which differs from the  $T$  dependence of the elastic modulus usually observed for solids, namely monotonic hardening with decreasing  $T$  [the inset in Fig. 1(b)] [51]. In  $C_B(T)$  [Fig. 1(a)], the Curie-type softening turns to hardening upon cooling from  $\sim 70$  K to  $\sim 50$  K,

and the elasticity rapidly recovers upon cooling below  $\sim 50$  K.

In the case of magnets, the Curie-type softening of the elastic modulus emerges as a precursor lattice instability to a structural transition, which is driven by the coupling of the lattice to the magnetic fluctuations [33,36–38,41,43–47]. For  $\text{LaCoO}_3$ , although there is no structural transition across the spin crossover [52], the Curie-type softening of  $C_B(T)$  [Fig. 1(a)] indicates the presence of isostructural lattice instability in the insulating paramagnetic state, which should arise from magnetic fluctuations. This symmetry-conserving isotropic lattice instability is compatible with the preservation of crystal symmetry across the spin crossover, which was microscopically observed in a NMR study [20]. For  $C_B(T)$  of  $\text{LaCoO}_3$  [Fig. 1(a)], the rapid recovery of the elasticity upon cooling below  $\sim 50$  K should arise from the evolution of the LS population, where the magnetic fluctuations are simultaneously quenched.

We note here that, for  $\text{LaCoO}_3$ , inelastic neutron scattering studies have indicated quasielastic magnetic scattering in the insulating paramagnetic state above  $\sim 100$  K and this gapless mode has been characterized as ferromagnetic fluctuations [14,26–28]. Thus, the Curie-type softening of  $C_B(T)$  for  $\text{LaCoO}_3$  should arise from the coupling between the ferromagnetic fluctuations and acoustic phonons. According to inelastic neutron scattering studies on  $\text{LaCoO}_3$ , the quasielastic magnetic scattering is suppressed in the insulating paramagnetic state below  $\sim 100$  K with the appearance of a 0.6-meV-gapped mode, and both the gapless and 0.6-meV-gapped modes disappear in the nonmagnetic state below  $\sim 30$  K [14,15,28], which is compatible with the cessation of Curie-type softening of  $C_B(T)$  for  $\text{LaCoO}_3$  below  $\sim 70$  K [Fig. 1(a)].

In contrast to  $C_B(T)$  (Fig. 1(a)), the tetragonal  $C_t(T)$  [Fig. 1(b)] and the trigonal  $C_{44}(T)$  [Fig. 1(c)] exhibit hardening upon cooling below 300 K. However, these hardenings of  $C_t(T)$  and  $C_{44}(T)$  are of a different type from usual hardening [51]. In usual solids, the elastic modulus hardens linearly with decreasing  $T$  at high temperatures, and hardens as  $\sim T^4$  at sufficiently low temperatures, which is hardening with convex  $T$  dependence [inset in Fig. 1(b)] [51].  $C_t(T)$  [Fig. 1(b)] and  $C_{44}(T)$  [Fig. 1(c)] of  $\text{LaCoO}_3$  behave differently from usual hardening [inset in Fig. 1(b)] in that although  $C_t(T)$  ( $C_{44}(T)$ ) exhibits  $T$ -linear hardening upon cooling from 300 K to  $\sim 220$  K ( $\sim 160$  K) [dashed lines in Figs. 1(b) and 1(c)], the  $T$  dependence starts to deviate upward from  $T$ -linear hardening below  $\sim 220$  K ( $\sim 160$  K), exhibits hardening with unusual concave  $T$  dependence from  $\sim 220$  K ( $\sim 160$  K) to  $\sim 30$  K, and saturates below  $\sim 30$  K [dotted lines in Figs. 1(b) and 1(c)].

For the spin-crossover cobaltite  $\text{LaCoO}_3$ , the phonon dispersion in the magnetic spin state and that in the nonmagnetic spin state should differ owing to their different electronic occupations of the Co-3d orbitals, and the initial slope of the acoustic phonon branch corresponding to the elastic constant should differ between the

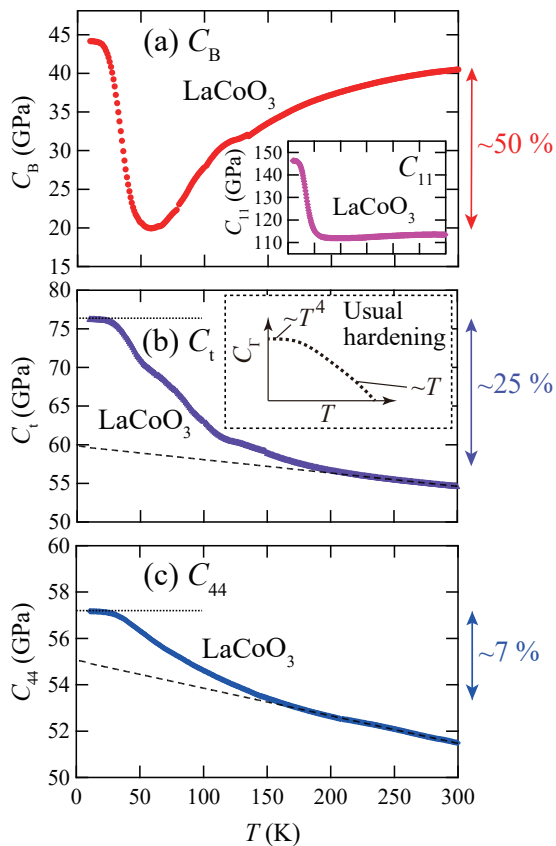


FIG. 1: (Color online) Elastic moduli of  $\text{LaCoO}_3$  as functions of  $T$ : (a)  $C_B(T)$ , (b)  $C_t(T)$ , and (c)  $C_{44}(T)$ . The inset in (a) depicts  $C_{11}(T)$  of  $\text{LaCoO}_3$ . The inset in (b) is a schematic of the  $T$  dependence of the elastic modulus usually observed for solids, namely monotonic hardening with decreasing  $T$  [51]. The dashed lines in (b) and (c) represent  $T$ -linear fits of the experimental data in the  $T$  range of 250–300 K, which are extrapolated to  $T = 0$  K. The dotted lines in (b) and (c) are guides to the eye, respectively indicating saturations of  $C_t(T)$  and  $C_{44}(T)$  below  $\sim 30$  K. The double arrow at the right side of (a) indicates the magnitude of the Curie-type softening of  $C_B(T)$ . The double arrows on the right sides of (b) and (c) respectively indicate the magnitudes of the hardening with concave  $T$  dependence of  $C_t(T)$  and  $C_{44}(T)$ .

magnetic spin state and nonmagnetic spin state. Thus, the occurrence of the spin crossover should give rise to an elasticity crossover between the magnetic spin state and nonmagnetic spin state. The unusual hardening with concave  $T$  dependence in  $C_t(T)$  [Fig. 1(b)] and  $C_{44}(T)$  [Fig. 1(c)] is most probably caused by the elasticity crossover arising from the spin crossover. Figure 2(a) is a schematic of the elasticity crossover in  $C_t(T)$  and  $C_{44}(T)$  of  $\text{LaCoO}_3$ , illustrating that upon cooling, a crossover from the magnetic-spin-state-dominant elasticity to the nonmagnetic-spin-state-dominant elasticity should occur. This elasticity crossover indicates that, for  $C_t(T)$  and  $C_{44}(T)$  of  $\text{LaCoO}_3$ , the magnetic-spin-state-dominant elasticity is softer than the nonmagnetic-spin-

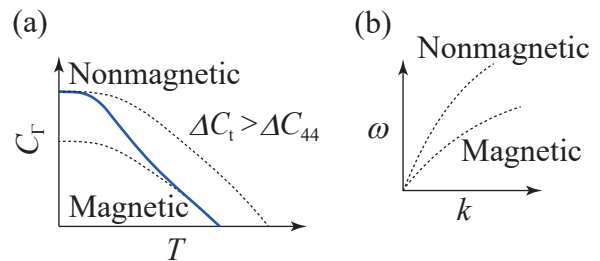


FIG. 2: (Color online) Schematics of (a) elasticity crossover between magnetic and nonmagnetic spin states in  $C_t(T)$  and  $C_{44}(T)$  of  $\text{LaCoO}_3$  and (b) acoustic phonon branches in magnetic and nonmagnetic spin states of  $\text{LaCoO}_3$ . The dotted curves in (a) schematically show the  $T$  dependence of magnetic-spin-state-dominant and nonmagnetic-spin-state-dominant elasticities.

state-dominant elasticity [dotted curves in Fig. 2(a)], which reflects that the initial slope of the acoustic phonon branch in the magnetic spin state is lower than that in the nonmagnetic spin state, as illustrated in Fig. 2(b).

For  $C_t(T)$  and  $C_{44}(T)$  of  $\text{LaCoO}_3$ , the magnitude of the unusual hardening with concave  $T$  dependence is larger in the tetragonal  $C_t(T)$  with  $E_g$  symmetry ( $\Delta C_t/C_t \sim 25\%$ ) [Fig. 1(b)] than in the trigonal  $C_{44}(T)$  with  $T_{2g}$  symmetry ( $\Delta C_{44}/C_{44} \sim 7\%$ ) [Fig. 1(c)]. This suggests that the occupation of the Co-3d  $e_g$  orbitals actively affects the elasticity, where the elasticity in the magnetic spin state becomes softer than that in the nonmagnetic spin state [dotted curves in Fig. 2(a)]. By the occupation of the extended  $e_g$  orbitals, the ionic volume in the magnetic spin state becomes larger than that in the nonmagnetic spin state [3]. This should make the elasticity in the magnetic spin state softer than that in the nonmagnetic spin state.

The experimental observations presented in Figs. 1(a)–1(c) reveal that the elastic moduli of the pseudocubic  $\text{LaCoO}_3$  exhibit two types of elastic-mode-dependent unusual  $T$  dependence upon cooling in the insulating paramagnetic state, namely Curie-type softening in  $C_B(T)$  and hardening with concave  $T$  dependence in  $C_t(T)$  and  $C_{44}(T)$ . In the present study, these unusual  $T$  dependences were also observed in the lightly Ni-doped  $\text{LaCoO}_3$  of  $\text{La}(\text{Co}_{0.99}\text{Ni}_{0.01})\text{O}_3$ . The relative shifts of  $C_t(T)$ ,  $C_{44}(T)$ , and  $C_B(T)$  of  $\text{LaCoO}_3$  and  $\text{La}(\text{Co}_{0.99}\text{Ni}_{0.01})\text{O}_3$  are compared in Figs. 3(a), 3(b), and 4(a), respectively. As seen in Figs. 3(a) and 3(b),  $C_t(T)$  and  $C_{44}(T)$  of  $\text{La}(\text{Co}_{0.99}\text{Ni}_{0.01})\text{O}_3$  exhibit hardening with concave  $T$  dependence, which is almost identical to the case for  $\text{LaCoO}_3$ . In  $C_B(T)$  of  $\text{La}(\text{Co}_{0.99}\text{Ni}_{0.01})\text{O}_3$  shown in Fig. 4(a), Curie-type softening is observed as in  $\text{LaCoO}_3$ . However, as seen in Fig. 4(a), the magnitude of the Curie-type softening in  $C_B(T)$  of  $\text{La}(\text{Co}_{0.99}\text{Ni}_{0.01})\text{O}_3$  ( $\Delta C_B/C_B \sim 25\%$ ) is suppressed relative to that of  $\text{LaCoO}_3$  ( $\Delta C_B/C_B \sim 50\%$ ).

We note here that, although  $\text{LaCoO}_3$  and  $\text{La}(\text{Co}_{0.99}\text{Ni}_{0.01})\text{O}_3$  are both semiconductors, the

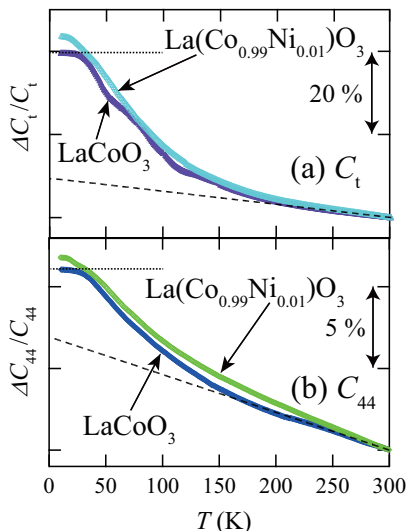


FIG. 3: (Color online) Relative shifts of (a)  $C_t(T)$  and (b)  $C_{44}(T)$  of  $\text{LaCoO}_3$  and  $\text{La}(\text{Co}_{0.99}\text{Ni}_{0.01})\text{O}_3$ . The experimental data of  $\text{LaCoO}_3$  and the dashed and dotted lines in (a) and (b) are identical to those in Figs. 1(b) and 1(c), respectively.

electrical resistivity of  $\text{La}(\text{Co}_{0.99}\text{Ni}_{0.01})\text{O}_3$  is much lower than that of  $\text{LaCoO}_3$ , indicating that the Ni-doping sensitively enhances the electron itinerancy in  $\text{LaCoO}_3$  [50]. Thus, the experimental observations shown in Figs. 3(a), 3(b), and 4(a) indicate that, while the hardening with concave  $T$  dependence of  $C_t(T)$  [Fig. 3(a)] and  $C_{44}(T)$  [Fig. 3(b)] is hardly affected by the enhancement of electron itinerancy, the Curie-type softening of  $C_B(T)$  [Fig. 4(a)] is sensitively suppressed with the enhancement of electron itinerancy.

As already mentioned in conjunction with Fig. 2, the hardening with concave  $T$  dependence in  $C_t(T)$  [Fig. 3(a)] and  $C_{44}(T)$  [Fig. 3(b)] should arise from the elasticity crossover that is driven by the spin crossover. Thus, the results shown in Figs. 3(a) and 3(b) indicate that the elasticity crossover occurs in  $\text{LaCoO}_3$  and  $\text{La}(\text{Co}_{0.99}\text{Ni}_{0.01})\text{O}_3$  identically, regardless of their different electron itinerancy. We note here that, for the Ni-doped  $\text{LaCoO}_3$  of  $\text{La}(\text{Co}_{1-x}\text{Ni}_x)\text{O}_3$ , the electrical resistivity rapidly decreases with an increasing Ni concentration  $x$  only below a few percent, which is considered to enable the insulator-to-metal transition at  $x \sim 0.4$  [49]. Thus, the effect of the enhanced electron itinerancy on the elasticity crossover is expected to emerge in  $\text{La}(\text{Co}_{1-x}\text{Ni}_x)\text{O}_3$  with a Ni concentration  $x$  increasing above  $x = 0.01$  ( $\text{La}(\text{Co}_{0.99}\text{Ni}_{0.01})\text{O}_3$ ).

In contrast to the elasticity crossover observed in  $C_t(T)$  (Fig. 3(a)) and  $C_{44}(T)$  (Fig. 3(b)), the Curie-type softening of  $C_B(T)$  is sensitively suppressed in  $\text{La}(\text{Co}_{0.99}\text{Ni}_{0.01})\text{O}_3$  relative to  $\text{LaCoO}_3$  [Fig. 4(a)], which should relate to the enhancement of electron itinerancy. As mentioned in the second and third paragraphs of this section, the Curie-type softening of  $C_B(T)$  for  $\text{LaCoO}_3$

indicates the presence of isostructural lattice instability in the insulating paramagnetic state, which should arise from the ferromagnetic fluctuations [14,15,28]. Thus, the results shown in Fig. 4(a) indicate that the ferromagnetic fluctuations are sensitively suppressed with the enhancement of electron itinerancy. For  $\text{LaCoO}_3$ , it has recently been claimed on the basis of inelastic neutron scattering and resonant inelastic X-ray scattering results that the ferromagnetic fluctuations in the insulating paramagnetic state are spin-state fluctuations emerging in the nearest-neighbor  $\text{Co}^{3+}$  pairs; i.e., the spin-state pair fluctuates between the HS-LS paired state and IS-IS paired state, which is called the HS-IS duality of the magnetic  $\text{Co}^{3+}$  ions [Fig. 4(b)] [28,29]. Thus, the present study suggests that the isostructural lattice instability in  $\text{LaCoO}_3$  [Fig. 1(a)] is driven by the HS-IS duality that is sensitive to the bond length between the nearest-neighbor  $\text{Co}^{3+}$  ions, and the HS-IS duality is sensitively suppressed with the enhancement of electron itinerancy [Fig. 4(a)].

For the HS-IS duality in  $\text{LaCoO}_3$ , an inelastic neutron scattering study revealed that, below 300 K, the spatial correlation robustly sustains the size corresponding to the seven Co sites that comprise one central Co site and its six nearest-neighbor Co sites [inset in Fig. 4(a)], and the Co-3d electrons are spatially delocalized within this seven-site unit [28]. It is thus suggested that the isostructural lattice instability in  $\text{LaCoO}_3$  [Fig. 1(a)] arises from the coupling of the lattice to the seven-Co-site clusters, within each of which the  $d$  electrons are confined but delocalized. Additionally, it is suggested for  $\text{LaCoO}_3$  that the delocalized electrons confined within the seven-Co-site clusters are released from the clusters by the Ni doping, where the HS-IS duality is suppressed in conjunction with the suppression of the isostructural lattice instability [Fig. 4(a)] and the enhancement of electron itinerancy.

Taking into account the HS-IS duality, we here analyze the Curie-type softening in  $C_B(T)$  of  $\text{LaCoO}_3$  and  $\text{La}(\text{Co}_{0.99}\text{Ni}_{0.01})\text{O}_3$  and further discuss this elastic anomaly. In magnets, the Curie-type softening emerges as a precursor to a structural transition, which is driven by the coupling of the lattice to the magnetic fluctuations [33,36–38,41–47]. A mean-field expression of the Curie-type softening in the temperature dependence of the elastic modulus  $C_\Gamma(T)$  is given as

$$C_\Gamma(T) = C_\Gamma^{(0)} \frac{T - T_c}{T - \theta}, \quad (1)$$

with  $C_\Gamma^{(0)}$  the background elastic constant,  $T_c$  the second-order critical temperature for elastic softening  $C_\Gamma \rightarrow 0$ , and  $\theta$  the intersite strain-sensitive magnetic interaction. Here,  $\theta$  is positive (negative) when the interaction is ferrodistorptive (antiferrodistorptive). In Fig. 4(a), fits of the experimental  $C_B(T)$  to Eq. (1) are depicted as solid curves, which follow the experimental data well. Values for the fitting parameters are listed in the table at the right side of Fig. 4(a).

From the fit for  $\text{LaCoO}_3$  [Fig. 4(a)], it is expected that

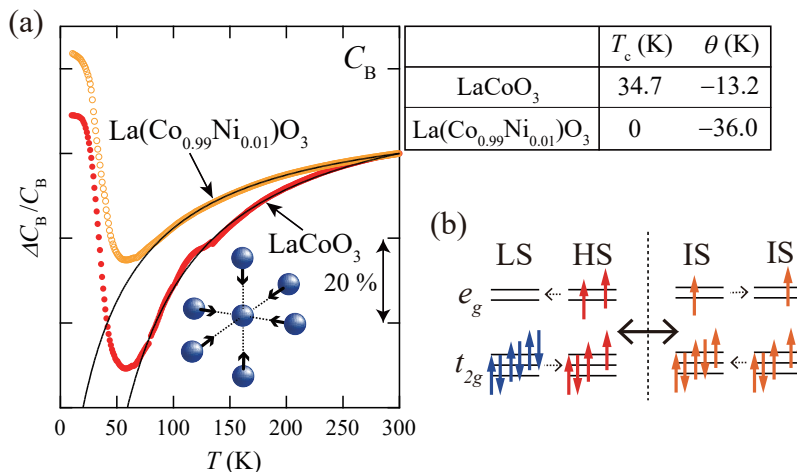


FIG. 4: (Color online) (a) The relative shifts of  $C_B(T)$  of LaCoO<sub>3</sub> and La(Co<sub>0.99</sub>Ni<sub>0.01</sub>)O<sub>3</sub>.  $C_B(T)$  of LaCoO<sub>3</sub> is identical to that in Fig. 1(a). The solid curves are fits of Eq. (1) to the experimental  $C_B(T)$ . Values of the fitting parameters are listed in the table at the right side of the figure. The inset is a schematic of the isostructural deformation of neighboring Co<sup>3+</sup> ions. (b) Schematic of the HS-IS duality of nearest-neighbor Co<sup>3+</sup> ions.

an isostructural phase transition occurs at  $T_c \sim 35$  K [table at the right side of Fig. 4(a)], with the transition being driven by the HS-IS duality. However, considering the cessation of the Curie-type softening in  $C_B(T)$  of LaCoO<sub>3</sub> below  $\sim 70$  K [Fig. 4(a)] and that there is no observation of a phase transition in the specific heat measurements [52], it is suggested that LaCoO<sub>3</sub> avoids the occurrence of the isostructural phase transition by entering the nonmagnetic LS state. We here note that recent high-magnetic-field magnetostriction studies of LaCoO<sub>3</sub> claimed the emergence of a spin-state-crystallized phase at high magnetic fields above  $\sim 70$  T and temperatures below  $\sim 30$  K, where a cubic superlattice of seven-IS-site clusters and LS ions is formed [31,32]. In Ref. [31,32], this spin-state crystallization is considered to originate from the HS-IS duality, where the  $d$  electrons of the seven-IS-site cluster are confined but delocalized within the cluster. The Curie-type softening in  $C_B(T)$  of LaCoO<sub>3</sub> might correspond to a precursor to the spin-state crystallization that is avoided in a zero magnetic field by entering the nonmagnetic LS state.

From the fit for La(Co<sub>0.99</sub>Ni<sub>0.01</sub>)O<sub>3</sub> [Fig. 4(a)], it is expected that the isostructural transition temperature  $T_c$  of La(Co<sub>0.99</sub>Ni<sub>0.01</sub>)O<sub>3</sub> is suppressed ( $T_c \sim 0$  K) relative to LaCoO<sub>3</sub> ( $T_c \sim 35$  K), while the intersite antiferrodistortive interaction  $\theta < 0$  is enhanced in La(Co<sub>0.99</sub>Ni<sub>0.01</sub>)O<sub>3</sub> ( $\theta \sim -36$  K) relative to LaCoO<sub>3</sub> ( $\theta \sim -13$  K) [table at the right side of Fig. 4(a)]. In the spin-crossover system,  $T_c$  in Eq. (1) should be determined by the onsite spin-state/strain coupling plus the intersite interaction  $\theta$ . Thus, the Ni doping dependence of  $T_c$  (suppression) being opposite to that of  $\theta$  (enhancement) indicates that  $T_c$  is dominantly determined by the onsite spin-state/strain coupling that is suppressed by Ni doping. Additionally, considering the formation

of the seven-Co-site spin-state clusters originating from the HS-IS duality, it is expected that the isostructural transition at  $T_c$  stabilizes the cluster-confined electronic state by contracting the clusters via the onsite spin-state/strain coupling [inset in Fig. 4(a)], but the Ni doping destabilizes this clustered state; i.e., it suppresses  $T_c$  and enhances the intersite antiferrodistortive interaction  $\theta$  in conjunction with the enhancement of electron itinerancy. Here the antiferrodistortive intersite interaction  $\theta$  favors the alternate arrangement of contracted and expanded lattice units. Thus, in the spin-crossover cobaltite LaCoO<sub>3</sub>, because the Co<sup>3+</sup> ionic volumes are different in the HS, IS, and LS states, it is expected that the antiferrodistortive intersite interaction  $\theta$  favors the alternate arrangement of the magnetic HS/IS and nonmagnetic LS Co<sup>3+</sup> ions. For La(Co<sub>1-x</sub>Ni<sub>x</sub>)O<sub>3</sub>, previous magnetization experiments revealed that the Ni-doping induces ferromagnetic behavior [49]. This might be relevant to the enhancement of the intersite antiferrodistortive interaction  $\theta$  with Ni doping in LaCoO<sub>3</sub>.

In LaCoO<sub>3</sub>, the application of pressure, namely the lattice contraction, is known to stabilize the nonmagnetic LS state [53,54]. Thus, the lattice expansion should conversely destabilize the nonmagnetic LS state, and the magnetic state should persist to lower temperatures. Consistently, the lattice-expanded LaCoO<sub>3</sub> of the tensile-strained thin film and the nanoparticles exhibits a ferromagnetic order, the transition temperature of which varies depending on the lattice expansion ( $T_C < \sim 90$  K) [55-66]. In LaCoO<sub>3</sub>, considering that  $T_C$  of the tensile-strained thin film increases with the tensile strain [62], it is expected that the paramagnetic state with the HS-IS duality emerges as a result of the competition between the nonmagnetic LS state and ferromagnetic ordered state.

#### IV. SUMMARY

Ultrasound velocity measurements of  $\text{LaCoO}_3$  and  $\text{La}(\text{Co}_{0.99}\text{Ni}_{0.01})\text{O}_3$  revealed two types of symmetry-resolved elastic anomaly in the insulating paramagnetic state that are commonly observed in these compounds. That in the bulk modulus  $C_B(T)$  indicated the presence of an isostructural lattice instability arising from the ferromagnetic fluctuations, and the other in the tetragonal  $C_t(T)$  and trigonal  $C_{44}(T)$  indicated the occurrence of elasticity crossover arising from the spin crossover. The present study also revealed that the isostructural lattice instability in  $\text{LaCoO}_3$  is sensitively suppressed by the Ni doping, indicating the suppression of the ferromagnetic fluctuations by the Ni doping in conjunction with the enhancement of electron itinerancy. This Ni doping effect can be explained on the basis that the ferromagnetic fluctuations originate from the HS-IS dual-

ity; i.e., the isostructural lattice instability arises from the coupling of the lattice to the seven-Co-site clusters within each of which the  $d$  electrons are confined but delocalized, and the Ni doping releases the cluster-confined electrons, leading to the suppression of the HS-IS duality in conjunction with the suppression of the isostructural lattice instability. The present study suggested that the spin-lattice coupling plays an important role in the emergence of the HS-IS duality in the spin-crossover cobaltite  $\text{LaCoO}_3$ .

#### V. ACKNOWLEDGMENTS

This work was partly supported by a Grant-in-Aid for Scientific Research (C) (Grant No. 21K03476) from MEXT of Japan.

- 
- \* Electronic address: watanabe.tadataka@nihon-u.ac.jp  
 † Present address: Nissan ARC Limited, Yokosuka, Kanagawa 237-0061, Japan
- <sup>1</sup> M. Imada, A. Fujimori, and Y. Tokura, *Rev. Mod. Phys.* **70**, 1039 (1998).
  - <sup>2</sup> R. Heikes, R. Miller, and R. Mazelsky, *Physica* **30**, 1600 (1964).
  - <sup>3</sup> K. Asai, A. Yoneda, O. Yokokura, J. M. Tranquada, G. Shirane, and K. Kohn, *J. Phys. Soc. Jpn.* **67**, 290 (1998).
  - <sup>4</sup> P. Gütlich, *Spin Crossover in Transition Metal Compounds I*, in *Top. Curr. Chem. Vol. 233-235*, edited by P. Gütlich and H. A. Goodwin (Springer, Berlin Heidelberg, 2004).
  - <sup>5</sup> J. Hohenberger, K. Ray, and K. Meyer, *Nat. Commun.* **3**, 720 (2012).
  - <sup>6</sup> S. I. Ohkoshi, K. Imoto, Y. Tsunobuchi, S. Takano, and H. Tokoro, *Nat. Chem.* **3**, 564 (2011).
  - <sup>7</sup> V. Krewald, M. Retegan, F. Neese, W. Lubitz, D. A. Pantazis, and N. Cox, *Inorg. Chem.* **55**, 488 (2016).
  - <sup>8</sup> S. Venkataramani, U. Jana, M. Dommaschk, F. D. Sönnichsen, F. Tuczek, and R. Herges, *Science* **331**, 445 (2011).
  - <sup>9</sup> R. Nomura, H. Ozawa, S. Tateno, K. Hirose, J. Hernlund, S. Muto, H. Ishii, and N. Hiraoka, *Nature (London)* **473**, 199 (2011).
  - <sup>10</sup> S. Ju, T.-Y. Cai, H.-S. Lu, and C.-D. Gong, *J. Am. Chem. Soc.* **134**, 13780 (2012).
  - <sup>11</sup> S. Noguchi, S. Kawamata, K. Okuda, H. Nojiri, and M. Motokawa, *Phys. Rev. B* **66**, 094404 (2002).
  - <sup>12</sup> Z. Ropka and R. J. Radwanski, *Phys. Rev. B* **67**, 172401 (2003).
  - <sup>13</sup> M. W. Haverkort, Z. Hu, J. C. Cezar, T. Burnus, H. Hartmann, M. Reuther, C. Zobel, T. Lorenz, A. Tanaka, N. B. Brookes, H. H. Hsieh, H.-J. Lin, C. T. Chen, and L. H. Tjeng, *Phys. Rev. Lett.* **97**, 176405 (2006).
  - <sup>14</sup> D. Phelan, D. Louca, S. Rosenkranz, S.-H. Lee, Y. Qiu, P. J. Chupas, R. Osborn, H. Zheng, J. F. Mitchell, J. R. D. Copley, J. L. Sarrao, and Y. Moritomo, *Phys. Rev. Lett.* **96**, 027201 (2006).
  - <sup>15</sup> A. Podlesnyak, S. Streule, J. Mesot, M. Medarde, E. Pomjakushina, K. Conder, A. Tanaka, M. W. Haverkort, and D. I. Khomskii, *Phys. Rev. Lett.* **97**, 247208 (2006).
  - <sup>16</sup> K. Knížek, Z. Jiráček, J. Hejtmánek, P. Novák, and W. Ku, *Phys. Rev. B* **79**, 014430 (2009).
  - <sup>17</sup> S. Asai, N. Furuta, R. Okazaki, Y. Yasui, and I. Terasaki, *Phys. Rev. B* **86**, 014421 (2012).
  - <sup>18</sup> S. Mukhopadhyay, M. W. Finnis, and N. M. Harrison, *Phys. Rev. B* **87**, 125132 (2013).
  - <sup>19</sup> K. Tomiyasu, J. Okamoto, H. Y. Huang, Z. Y. Chen, E. P. Sinaga, W. B. Wu, Y. Y. Chu, A. Singh, R.-P. Wang, F. M. F. de Groot, A. Chainani, S. Ishihara, C. T. Chen, and D. J. Huang, *Phys. Rev. Lett.* **119**, 196402 (2017).
  - <sup>20</sup> Y. Shimizu, T. Takahashi, S. Yamada, A. Shimokata, T. Jin-no, and M. Itoh, *Phys. Rev. Lett.* **119**, 267203 (2017).
  - <sup>21</sup> M. A. Korotin, S. Y. Ezhov, I. V. Solovyev, V. I. Anisimov, D. I. Khomskii, and G. A. Sawatzky, *Phys. Rev. B* **54**, 5309 (1996).
  - <sup>22</sup> T. Mizokawa and A. Fujimori, *Phys. Rev. B* **54**, 5368 (1996).
  - <sup>23</sup> T. Saitoh, T. Mizokawa, A. Fujimori, M. Abbate, Y. Takeda, and M. Takano, *Phys. Rev. B* **55**, 4257 (1997).
  - <sup>24</sup> S. Yamaguchi, Y. Okimoto, and Y. Tokura, *Phys. Rev. B* **55**, R8666 (1997).
  - <sup>25</sup> A. Ishikawa, J. Nohara, and S. Sugai, *Phys. Rev. Lett.* **93**, 136401 (2004).
  - <sup>26</sup> K. Asai, P. Gehring, H. Chou, and G. Shirane, *Phys. Rev. B* **40**, 10982 (1989).
  - <sup>27</sup> K. Asai, O. Yokokura, N. Nishimori, H. Chou, J. M. Tranquada, G. Shirane, S. Higuchi, Y. Okajima, and K. Kohn, *Phys. Rev. B* **50**, 3025 (1994).
  - <sup>28</sup> K. Tomiyasu, T. Nomura, Y. Kobayashi, S. Ishihara, S. Ohira-Kawamura, and M. Kofu, arXiv: 1808.05888.
  - <sup>29</sup> A. Hariki, R.-P. Wang, A. Sotnikov, K. Tomiyasu, D. Betto, N. B. Brookes, Y. Uemura, M. Ghiasi, F. M. F. de Groot, and J. Kuneš, *Phys. Rev. B* **101**, 245162 (2020).
  - <sup>30</sup> H. Park, R. Nanguneri, and A. T. Ngo, *Phys. Rev. B* **101**, 195125 (2020).
  - <sup>31</sup> A. Ikeda, Y. H. Matsuda, and K. Sato, *Phys. Rev. Lett.* **125**, 177202 (2020).
  - <sup>32</sup> A. Ikeda, Y. H. Matsuda, K. Sato, Y. Ishii, H. Sawabe, D. Nakamura, S. Takeyama, and J. Nasu, arXiv: 2201.02704.

- <sup>33</sup> B. Lüthi, *Physical Acoustics in the Solid State* (Springer, 2005).
- <sup>34</sup> T. Watanabe, S. Hara, and S. Ikeda, *Phys. Rev. B* **78**, 094420 (2008).
- <sup>35</sup> T. Watanabe, S. Hara, S. Ikeda, and K. Tomiyasu, *Phys. Rev. B* **84**, 020409(R) (2011).
- <sup>36</sup> T. Watanabe, S. Ishikawa, H. Suzuki, Y. Kousaka, and K. Tomiyasu, *Phys. Rev. B* **86**, 144413 (2012).
- <sup>37</sup> Y. Nii, N. Abe, and T. Arima, *Phys. Rev. B* **87**, 085111 (2013).
- <sup>38</sup> T. Watanabe, T. Ishikawa, S. Hara, A. T. M. N. Islam, E. M. Wheeler, and B. Lake, *Phys. Rev. B* **90**, 100407(R) (2014).
- <sup>39</sup> T. Watanabe, S. Takita, K. Tomiyasu, and K. Kamazawa, *Phys. Rev. B* **92**, 174420 (2015).
- <sup>40</sup> T. Watanabe, S. Yamada, R. Koborinai, and T. Katsufuji, *Phys. Rev. B* **96**, 014422 (2017).
- <sup>41</sup> T. Watanabe, S. Kobayashi, Y. Hara, J. Xu, B. Lake, J.-Q. Yan, A. Niazi, and D. C. Johnston, *Phys. Rev. B* **98**, 094427 (2018).
- <sup>42</sup> T. Watanabe, H. Kato, Y. Hara, J. W. Krizan, and R. J. Cava, *Phys. Rev. B* **101**, 214425 (2020).
- <sup>43</sup> Y. Kino, B. Lüthi, and M. E. Mullen, *J. Phys. Soc. Jpn.* **33**, 687 (1972); *Solid State Commun.* **12**, 275 (1973).
- <sup>44</sup> M. Kataoka and J. Kanamori, *J. Phys. Soc. Jpn.* **32**, 113 (1972).
- <sup>45</sup> H. Hazama, T. Goto, Y. Nemoto, Y. Tomioka, A. Asamitsu, and Y. Tokura, *Phys. Rev. B* **62**, 15012 (2000).
- <sup>46</sup> B. Kindler, D. Finsterbusch, R. Graf, F. Ritter, W. Assmus, and B. Lüthi, *Phys. Rev. B* **50**, 704 (1994).
- <sup>47</sup> B. J. Ramshaw, A. Shekhter, R. D. McDonald, J. B. Betts, J. N. Mitchell, P. H. Tobash, C. H. Mielke, E. D. Bauer, and A. Migliori, *PNAS* **112**, 3285 (2015).
- <sup>48</sup> T. S. Naing, T. Kobayashi, Y. Kobayashi, M. Suzuki, and K. Asai, *J. Phys. Soc. Jpn.* **75**, 084601 (2006).
- <sup>49</sup> D. Hammer, J. Wu, and C. Leighton, *Phys. Rev. B* **69**, 134407 (2004).
- <sup>50</sup> K. Tomiyasu, Y. Kubota, S. Shimomura, M. Onodera, S. I. Koyama, T. Nojima, S. Ishihara, H. Nakao, and Y. Murakami, *Phys. Rev. B* **87**, 224409 (2013).
- <sup>51</sup> Y. P. Varshni, *Phys. Rev. B* **2**, 3952 (1970).
- <sup>52</sup> T. Kyômen, Y. Asaka, and M. Itoh, *Phys. Rev. B* **67**, 144424 (2003).
- <sup>53</sup> D. P. Kozlenko, N. O. Golosova, Z. Jiráček, L. S. Dubrovinsky, B. N. Savenko, M. G. Tucker, Y. Le Godec, and V. P. Glazkov, *Phys. Rev. B* **75**, 064422 (2007).
- <sup>54</sup> K. Knížek, Z. Jiráček, J. Hejtmánek, M. Veverka, M. Maryško, G. Maris, and T. T. M. Palstra, *Eur. Phys. J. B* **47**, 213 (2005).
- <sup>55</sup> D. Fuchs, C. Pinta, T. Schwarz, P. Schweiss, P. Nagel, S. Schuppler, R. Schneider, M. Merz, G. Roth, and H. v. Löhneysen, *Phys. Rev. B* **75**, 144402 (2007).
- <sup>56</sup> D. Fuchs, E. Arac, C. Pinta, S. Schuppler, R. Schneider, and H. v. Löhneysen, *Phys. Rev. B* **77**, 014434 (2008).
- <sup>57</sup> J. W. Freeland, J. X. Ma, and J. Shi, *Appl. Phys. Lett.* **93**, 212501 (2008).
- <sup>58</sup> V. V. Mehta, M. Liberati, F. J. Wong, R. V. Chopdekar, E. Arenholz, and Y. Suzuki, *J. Appl. Phys.* **105**, 07E503 (2009).
- <sup>59</sup> A. D. Rata, A. Herklotz, L. Schultz, and K. Dörr, *Eur. Phys. J. B* **76**, 215 (2010).
- <sup>60</sup> W. S. Choi, J.-H. Kwon, H. Jeon, J. E. Hamann-Borrero, A. Radi, S. Macke, R. Sutarto, F. He, G. A. Sawatzky, V. Hinkov, M. Kim, and H. N. Lee, *Nano Lett.* **12**, 4966 (2012).
- <sup>61</sup> J. Fujioka, Y. Yamasaki, H. Nakao, R. Kumai, Y. Murakami, M. Nakamura, M. Kawasaki, and Y. Tokura, *Phys. Rev. Lett.* **111**, 027206 (2013).
- <sup>62</sup> J. Fujioka, Y. Yamasaki, A. Doi, H. Nakao, R. Kumai, Y. Murakami, M. Nakamura, M. Kawasaki, T. Arima, and Y. Tokura, *Phys. Rev. B* **92**, 195115 (2015).
- <sup>63</sup> Y. Yamasaki, J. Fujioka, H. Nakao, J. Okamoto, T. Suda, Y. Murakami, M. Nakamura, M. Kawasaki, T. Arima, and Y. Tokura, *J. Phys. Soc. Jpn.* **85**, 023704 (2016).
- <sup>64</sup> G. E. Sterbinsky, R. Nanguneri, J. X. Ma, J. Shi, E. Karapetrova, J. C. Woicik, H. Park, J.-W. Kim, and P. J. Ryan, *Phys. Rev. Lett.* **120**, 197201 (2018).
- <sup>65</sup> Y. Yokoyama, Y. Yamasaki, M. Taguchi, Y. Hirata, K. Takubo, J. Miyawaki, Y. Harada, D. Asakura, J. Fujioka, M. Nakamura, H. Daimon, M. Kawasaki, Y. Tokura, and H. Wadati, *Phys. Rev. Lett.* **120**, 206402 (2018).
- <sup>66</sup> S. Zhou, L. Shi, J. Zhao, L. He, H. Yang, and S. Zhang, *Phys. Rev. B* **76**, 172407 (2007).